

The Physics of K^0 - \bar{K}^0 Mixing: \hat{B}_K and ΔM_{LS} in the Chiral Quark Model

V. Antonelli, S. Bertolini, M. Fabbrichesi and E.I. Lashin[†]

INFN, Sezione di Trieste

and

Scuola Internazionale Superiore di Studi Avanzati

via Beirut 4, I-34013 Trieste, Italy.

Abstract

We compute the \hat{B}_K parameter and the mass difference ΔM_{LS} of the K^0 - \bar{K}^0 system by means of the chiral quark model. The chiral coefficients of the relevant $\Delta S = 2$ and $\Delta S = 1$ chiral lagrangians are computed via quark-loop integration. We include the relevant effects of one-loop corrections in chiral perturbation theory. The final result is very sensitive to non-factorizable corrections of $O(\alpha_S N)$ coming from gluon condensation. The size of the gluon condensate is determined by fitting the experimental value of the amplitude $K^+ \rightarrow \pi^+ \pi^0$. By varying all the relevant parameters we obtain

$$\hat{B}_K = 0.87^{+0.33}_{-0.23}.$$

We evaluate within the model the long-distance contributions to ΔM_{LS} induced by the double insertion of the $\Delta S = 1$ chiral lagrangian and study the interplay between short- and long-distance amplitudes. By varying all parameters we obtain

$$\Delta M_{LS}^{th} / \Delta M_{LS}^{exp} = 0.76^{+0.64}_{-0.34}.$$

Finally, we investigate the phenomenological constraints on the Kobayashi-Maskawa parameter $\text{Im } \lambda_t$ entering the determination of ε'/ε .

SISSA 20/96/EP

September 1996

[†]Permanent address: Ain Shams University, Faculty of Science, Dept. of Physics, Cairo, Egypt.

The mixing in the K^0 - \bar{K}^0 system is determined by the weak effective hamiltonian through the mass matrix $\langle \bar{K}^0 | \mathcal{H}_W | K^0 \rangle$. Its computation requires both long- and short-distance physics. For this reason, the CP violating quantity ε and the mass difference ΔM_{LS} , which are respectively related to the imaginary and the real part of the mass matrix, are factorized in the renormalization-group invariant parameter \hat{B}_K , which takes into account long-distance effects, and the Wilson coefficients, which account for the short distance ones. ΔM_{LS} receives in addition a long-distance correction from the double insertion of the $\Delta S = 1$ hamiltonian.

In this work we apply the chiral quark model [1](χ QM) and chiral perturbation techniques to estimate the long-distance part of the mass matrix. Such an analysis follows our recent studies of the $\Delta I = 1/2$ selection rule [2] and ε'/ε [3] within the χ QM approach to kaon physics.

The long-distance contributions thus computed are eventually matched to an up-to-date next-to-leading order (NLO) determination of the short-distance coefficients and the results compared with the experimental values.

1 INTRODUCTION

The effective $\Delta S = 2$ quark lagrangian at scales $\mu < m_c$ is given by

$$\mathcal{L}_{\Delta S=2} = -\frac{G_F^2 M_W^2}{4\pi^2} \left[\lambda_c^2 \eta_1 S(x_c) + \lambda_t^2 \eta_2 S(x_t) + 2\lambda_c \lambda_t \eta_3 S(x_c, x_t) \right] b(\mu) Q_{S2}(\mu), \quad (1.1)$$

where G_F is the Fermi constant, M_W is the W boson mass, $x_i = m_i^2/M_W^2$, and μ is the renormalization scale. The parameters $\lambda_j = V_{jd}V_{js}^*$ represent the relevant combinations of Kobayashy-Maskawa (KM) matrix elements ($j = u, c, t$). Finally we denote by Q_{S2} the $\Delta S = 2$ local four quark operator

$$Q_{S2} = (\bar{s}_L \gamma^\mu d_L)(\bar{s}_L \gamma_\mu d_L). \quad (1.2)$$

The integration of the electroweak loops leads to the Inami-Lim functions [4]

$$S(x) = x \left[\frac{1}{4} + \frac{9}{4} \frac{1}{1-x} - \frac{3}{2} \frac{1}{(1-x)^2} \right] - \frac{3}{2} \left[\frac{x}{1-x} \right]^3 \ln x, \quad (1.3)$$

$$S(x_c, x_t) = -x_c \ln x_c + x_c \left[\frac{x_t^2 - 8x_t + 4}{4(1-x_t)^2} \ln x_t + \frac{3}{4} \frac{x_t}{x_t - 1} \right] \quad (1.4)$$

which depend on the masses of the charm and top quarks and describe the $\Delta S = 2$ transition amplitude in the absence of strong interactions.

The short-distance QCD corrections are encoded in the coefficients η_1 , η_2 and η_3 with a common scale-dependent factor $b(\mu)$ factorized out. They are functions of the heavy quarks masses and of the scale parameter Λ_{QCD} . These QCD corrections are available to NLO [5, 6, 7] in the strong and electromagnetic couplings.

The scale-dependent common factor of the short-distance corrections is given by

$$b(\mu) = [\alpha_s(\mu)]^{-2/9} \left(1 - J_3 \frac{\alpha_s(\mu)}{4\pi} \right), \quad (1.5)$$

where J_3 depends on the γ_5 -scheme used in the regularization. The naive dimensional regularization (NDR) gives

$$J_3^{\text{NDR}} = -\frac{307}{162}, \quad (1.6)$$

while in the 't Hooft-Veltman (HV) scheme one finds

$$J_3^{\text{HV}} = -\frac{91}{162}. \quad (1.7)$$

For the running QCD coupling we take the average over recent LEP and SLC determinations [8],

$$\alpha_s(m_Z) = 0.119 \pm 0.006 \quad (1.8)$$

which corresponds to

$$\Lambda_{\text{QCD}}^{(4)} = 350 \pm 100 \text{ MeV}. \quad (1.9)$$

The scale-dependent $B_K(\mu)$ parameter is defined by the matrix element

$$\langle \bar{K}^0 | Q_{S2}(\mu) | K^0 \rangle = \frac{4}{3} f_K^2 m_K^2 B_K(\mu), \quad (1.10)$$

where f_K and m_K are the kaon decay constant and mass, respectively (see table 2 for their numerical values).

The value of $B_K(\mu)$ measures the deviation of the matrix element from the vacuum saturation approximation used in the original work of Gaillard and Lee [9], namely $B_K(\mu) = 1$. The physically relevant parameter is \hat{B}_K , which is defined by the relation:

$$\hat{B}_K = B_K(\mu) b(\mu). \quad (1.11)$$

\hat{B}_K	Method	Reference
$3/4$	Leading $1/N_c$	[11]
0.37	Lowest-Order Chiral Perturbation Theory	[12]
0.70 ± 0.10	Next-to-Leading $1/N_c$ Estimate	[13]
0.4 ± 0.2	Next-to-Leading $1/N_c$ Estimate, $O(p^2)$	[14]
0.42 ± 0.06	$O(p^4)$ CHPT + $1/N_c$ Estimate	[15]
0.39 ± 0.10	QCD-Hadronic Duality	[16, 17]
$0.5 \pm 0.1 \pm 0.2$	QCD Sum Rules (3-Point Functions)	[18]
0.825 ± 0.035	Lattice (Quenched Approximation)	[19]

Table 1: Values of \hat{B}_K obtained in different approaches (from ref. [10]).

This quantity should be in principle renormalization scale independent. As we include the perturbative NLO determination of the Wilson coefficient, we shall also discuss the γ_5 -scheme dependence of our result.

An useful up-to-date summary of various determinations of this parameter is given in Table 1 which is taken from ref. [10].

We have followed the approach described in ref. [20] in which the weak chiral lagrangian is considered as the effective theory of the χ QM [1]. In the present case, it is the bosonization of the operator Q_{S2} and the determination of the coefficient of the corresponding $\Delta S = 2$ chiral lagrangian that is made possible by the χ QM.

In the determination of $B_K(\mu)$ to $O(\alpha_s N_c)$ enters the contribution of the gluon condensate. The final estimate is very sensitive to the value of such an input parameter. In order to restrict the range of allowed values, we impose the additional constraint of taking for the gluon condensate the value that gives the best fit of the experimental amplitude $K^+ \rightarrow \pi^+ \pi^0$, which is related at the leading order in chiral perturbation theory to that of $K^0 \rightarrow \bar{K}^0$. Such a procedure is consistent with that followed in ref. [2] where we reproduced the $\Delta I = 1/2$ rule by a similar choice of input parameters.

A long-distance scale dependence is introduced by the one-loop chiral corrections to the hadronic matrix elements. In principle, this scale dependence should match that in the Wilson coefficients and provides a scale independent value of \hat{B}_K . In practice, we find that there cannot be matching at this order insofar as both the

Wilson coefficient and the chiral corrections renormalize the parameter in the same direction. The scale dependence remains however below 20% and the final estimate is thus still reliable.

Our approach is in principle sensitive to the scheme used to treat γ_5 matrices in a generic space-time dimension. The NDR prescription of ref. [21, 22] preserves the chiral properties of the operator Q_{S2} by means of a convenient normalization of the evanescent operators. As discussed in ref. [20], the consistency with such a prescription makes the matrix elements of Q_{S2} the same in the two schemes. As a consequence, the remnant scheme dependence of the final result is that present in the short-distance factor $b(\mu)$.

There are two important parameters related to the K^0 - \bar{K}^0 mixing: the CP violating quantity ε which is proportional to the imaginary part of the mass matrix and the mass difference $\Delta M_{LS} \equiv m_L - m_S$. The observed value for these quantities are [23]:

$$|\varepsilon| = (2.266 \pm 0.023) \times 10^{-3} \quad (1.12)$$

and

$$\Delta M_{LS} = (3.510 \pm 0.018) \times 10^{-15} \text{ GeV}. \quad (1.13)$$

Knowing ε , we can determine $\text{Im } \lambda_t$, as discussed in section 6. As a by-product of the computation one also obtains an estimate for the width difference $\Delta \Gamma_{LS}$, the experimental value of which is

$$\Delta \Gamma_{LS} = -(7.374 \pm 0.010) \times 10^{-15} \text{ GeV}. \quad (1.14)$$

However, a consistent determination of this quantity requires one extra order in perturbation theory, as we shall discuss below.

From the theoretical point of view, the $K^0 - \bar{K}^0$ mass matrix can be written, using CPT invariance, as

$$\begin{aligned} \mathcal{M} &= \frac{1}{2m_K} \begin{pmatrix} \langle K^0 | H_W | K^0 \rangle & \langle K^0 | H_W | \bar{K}^0 \rangle \\ \langle \bar{K}^0 | H_W | K^0 \rangle & \langle \bar{K}^0 | H_W | \bar{K}^0 \rangle \end{pmatrix} \\ &= \begin{pmatrix} M - \frac{1}{2}i\Gamma & M_{12} - \frac{1}{2}i\Gamma_{12} \\ M_{12}^* - \frac{1}{2}i\Gamma_{12}^* & M - \frac{1}{2}i\Gamma \end{pmatrix} \end{aligned} \quad (1.15)$$

In the presence of CP violation ($\varepsilon \neq 0$) M_{12} and Γ_{12} are complex numbers. The diagonalization of the mass matrix (1.15) leads to the physical states:

$$\begin{aligned} K_L &= \frac{1}{\sqrt{2(1+|\varepsilon|^2)}} \left[K^0(1+\varepsilon) + \bar{K}^0(1-\varepsilon) \right] \\ K_S &= \frac{1}{\sqrt{2(1+|\varepsilon|^2)}} \left[K^0(1+\varepsilon) - \bar{K}^0(1-\varepsilon) \right] \end{aligned} \quad (1.16)$$

For a tiny CP violation, their associated mass and width differences are given by:

$$\Delta M_{LS} = \frac{1}{m_K} \text{Re} \left[\langle K^0 | H_W | \bar{K}^0 \rangle \right], \quad (1.17)$$

$$\Delta \Gamma_{LS} = - \frac{2}{m_K} \text{Im} \left[\langle K^0 | H_W | \bar{K}^0 \rangle \right]. \quad (1.18)$$

In order to estimate these two parameters we need to evaluate in addition to the quark box-diagram contribution, coming from the $\Delta S = 2$ effective weak lagrangian given in (1.1), the long-distance contribution coming from the double insertion of the $\Delta S = 1$ weak chiral lagrangian. In the latter case, the mixing between K^0 and \bar{K}^0 can proceed, up to the one-loop level, via one- and two-particle intermediate states

$$K^0 \rightarrow (\pi^0, \eta) \rightarrow \bar{K}^0, \quad (1.19)$$

$$K^0 \rightarrow (\pi^+ \pi^-, K^+ K^-, \pi^0 \pi^0, \eta \eta, \pi^0 \eta) \rightarrow \bar{K}^0, \quad (1.20)$$

Within the χ QM approach the $\Delta S = 1$ weak chiral lagrangian can be systematically derived at a given order in momentum expansion starting from the effective quark lagrangian [24]:

$$\mathcal{L}_{\Delta S=1} = - \frac{G_F}{\sqrt{2}} V_{ud} V_{us}^* \sum_i \left[z_i(\mu) + \tau y_i(\mu) \right] Q_i(\mu), \quad (1.21)$$

where Q_i are local four-quark operators obtained by integrating out in the standard model the vector bosons and the heavy quarks t , b and c . A convenient and by now standard basis includes the following ten quark operators:

$$\begin{aligned} Q_1 &= (\bar{s}_\alpha u_\beta)_{V-A} (\bar{u}_\beta d_\alpha)_{V-A}, \\ Q_2 &= (\bar{s}u)_{V-A} (\bar{u}d)_{V-A}, \\ Q_{3,5} &= (\bar{s}d)_{V-A} \sum_q (\bar{q}q)_{V \mp A}, \\ Q_{4,6} &= (\bar{s}_\alpha d_\beta)_{V-A} \sum_q (\bar{q}_\beta q_\alpha)_{V \mp A}, \\ Q_{7,9} &= \frac{3}{2} (\bar{s}d)_{V-A} \sum_q \hat{e}_q (\bar{q}q)_{V \pm A}, \\ Q_{8,10} &= \frac{3}{2} (\bar{s}_\alpha d_\beta)_{V-A} \sum_q \hat{e}_q (\bar{q}_\beta q_\alpha)_{V \pm A}, \end{aligned} \quad (1.22)$$

where α, β denote color indices ($\alpha, \beta = 1, \dots, N_c$) and \hat{e}_q are quark charges. Color indices for the color singlet operators are omitted. ($V \pm A$) refer to $\gamma_\mu(1 \pm \gamma_5)$. We recall that $Q_{1,2}$ stand for the W -induced current–current operators, Q_{3-6} for the QCD penguin operators and Q_{7-10} for the electroweak penguin (and box) ones.

The functions $z_i(\mu)$ and $y_i(\mu)$ are the Wilson coefficients and V_{ij} the KM matrix elements; $\tau = -V_{td}V_{ts}^*/V_{ud}V_{us}^*$.

In a previous work [20] we have computed the chiral coefficients for the complete $O(p^2)$ $\Delta S = 1$ chiral lagrangian. We will make use of those results to evaluate the long-distance contributions in eqs. (1.19)–(1.20).

2 A MODEL INDEPENDENT ESTIMATE OF \hat{B}_K

The $\Delta S = 2$ matrix element can be related via chiral symmetry to that of the $\Delta S = 1$ and $\Delta I = 3/2$ amplitude $\mathcal{A}(K^+ \rightarrow \pi^+\pi^0)$ [12]. Neglecting the $SU(3)$ breaking effects related to the chiral loop corrections to the matrix element, the electromagnetic contributions and the $\pi - \eta$ mixing, we obtain the relation

$$\frac{4}{3}f_K^2m_K^2\hat{B}_K = \frac{\sqrt{2}}{G_F} \frac{f_\pi}{V_{us}^*V_{ud}} \frac{m_K^2}{m_K^2 - m_\pi^2} \frac{b(\mu)}{z_1(\mu) + z_2(\mu)} \mathcal{A}(K^+ \rightarrow \pi^+\pi^0) . \quad (2.1)$$

In the previous equation V_{us} and V_{ud} are two matrix elements of the KM mixing matrix, $b(\mu)$ is the $\Delta S = 2$ Wilson coefficient given by (1.5), while $z_1(\mu)$ and $z_2(\mu)$ are the real parts of the Wilson coefficients for the two $\Delta S = 1$ operators Q_1 and Q_2 which dominate the $K^+ \rightarrow \pi^+\pi^0$ transition.

By inputting the experimental value $\mathcal{A}(K^+ \rightarrow \pi^+\pi^0) = 1.84 \times 10^{-8}$ GeV and the NLO results for the Wilson coefficients (the ratio $b(\mu)/(z_1(\mu) + z_2(\mu))$ is to a large extent μ and γ_5 -scheme independent) we find the model “independent” estimate

$$\hat{B}_K = 0.40 . \quad (2.2)$$

This number updates the value $\hat{B}_K = 0.33$ given in ref. [12].

On the other hand, having a model that reproduces the experimental result, in order to apply correctly eq. (2.1) we must subtract in $\mathcal{A}(K^+ \rightarrow \pi^+\pi^0)$ all the chiral symmetry breaking corrections due to chiral loops, electroweak penguins and $\pi - \eta$ mixing [2]. In this way we obtain in the χ QM approach, on the basis of chiral symmetry arguments alone, the following $O(p^2)$ prediction:

$$\hat{B}_K = \frac{3}{4}b(\mu) \frac{f_\pi f}{f_K^2} \left[1 + \frac{1}{N_c} (1 - \delta_{\langle GG \rangle}) \right] . \quad (2.3)$$

In the previous formula we have denoted by $\delta_{\langle GG \rangle}$ the non-perturbative gluonic corrections which arise in the χ QM approach,

$$\delta_{\langle GG \rangle} = \frac{N_c}{2} \frac{\langle \alpha_s GG / \pi \rangle}{16\pi^2 f^4}, \quad (2.4)$$

where $\langle \alpha_s GG / \pi \rangle$ is the gluon condensate and N_c is the number of colors. We will come back to these corrections in the next section.

In considering eq. (2.3) it is important to remember that the factor f_π comes from the soft pion theorem, while f is the chiral lagrangian parameter appearing in the calculation of the amplitude $\mathcal{A}(K^+ \rightarrow \pi^+\pi^0)$. At the tree level $f = f_\pi$. The spurious μ dependence present in eq. (2.3) should be canceled by that of the hadronic matrix elements, which is absent at the lowest order in the chiral expansion.

If we choose for the gluon condensate the value $\langle \alpha_s GG / \pi \rangle = (360 \text{ MeV})^4$ (which gives the best fit of $\mathcal{A}(K^+ \rightarrow \pi^+\pi^0)$), we obtain at $\mu = 0.8 \text{ GeV}$

$$\hat{B}_K \simeq 0.33. \quad (2.5)$$

This value includes the non-factorizable effects of gluon condensate corrections, which play a crucial role in the fit of the $\Delta I = 3/2$ amplitude in $K \rightarrow \pi\pi$ decays.

The value in eq. (2.5) represents the starting point of our analysis, to which we will add the effect of chiral loop contributions to the $\Delta S = 2$ matrix element.

3 COMPUTING B_K

In this section we will extend the techniques that we have developed for $\Delta S = 1$ weak processes in ref. [20], by using the χ QM to construct the $\Delta S = 2$ weak chiral lagrangian.

3.1 THE LEADING CHIRAL COEFFICIENT IN THE CHIRAL QUARK MODEL

At the leading $O(p^2)$ order in the chiral expansion, the strong interaction between the $SU(3)$ Goldstone bosons is described by the following effective lagrangian [25]

$$\mathcal{L}_{\text{strong}}^{(2)} = \frac{f^2}{4} \text{Tr} \left(D_\mu \Sigma D^\mu \Sigma^\dagger \right) + \frac{f^2}{2} B_0 \text{Tr} \left(\mathcal{M} \Sigma^\dagger + \Sigma \mathcal{M}^\dagger \right), \quad (3.1)$$

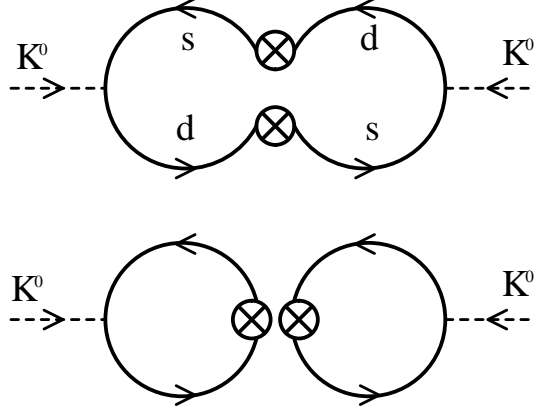


Figure 1: The two configurations relevant to the determination of the chiral coefficient $C(Q_{S2})$. The crossed circles stand for the insertion of the currents of the local $\Delta S = 2$ four-quark operator.

where \mathcal{M} is the mass matrix of the three light quarks (u,d and s) and Σ is defined as

$$\Sigma \equiv \exp \left(\frac{2i}{f} \Pi(x) \right), \quad \Pi(x) = \sum_{a=1..8} \lambda_a \pi^a(x)/2. \quad (3.2)$$

To the same order, the $\Delta S = 2$ weak chiral lagrangian is given by:

$$\mathcal{L}_{\Delta S=2}^{(2)} = C(Q_{S2}) \text{Tr} \left(\lambda_2^3 \Sigma D_\mu \Sigma^\dagger \right) \text{Tr} \left(\lambda_2^3 \Sigma D^\mu \Sigma^\dagger \right). \quad (3.3)$$

In eq. (3.3) D_μ indicates the covariant derivative with respect to any external field, while λ_2^3 is a combination of the $SU(3)$ Gell-Mann matrices which acts in the flavor space causing a transition from a d -quark to an s -quark: $(\lambda_2^3)_{lk} = \delta_{3l}\delta_{2k}$.

$C(Q_{S2})$ is the chiral coefficient, which we determine by comparison with the χ QM calculation. Two configurations contribute to the determination of this coefficient at $O(N_c)$, as shown in Fig. 1.

In both HV and NDR schemes we find (for convenience we do not write the overall $\Delta S = 2$ Wilson coefficient given in eq. (1.1))

$$C(Q_{S2}) = -\frac{f^4}{4} \left(1 + \frac{1}{N_c} \right). \quad (3.4)$$

An important correction to eq. (3.4) arises by considering the propagation of quarks in an external gluon field. The effects of non-perturbative gluonic corrections have been first studied in [14].

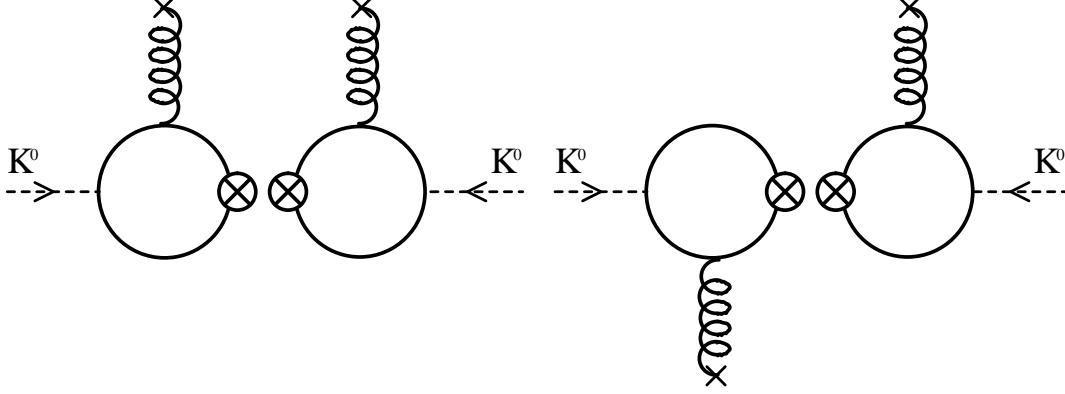


Figure 2: Same as Fig. 1 with the inclusion of the gluon corrections.

In the case of $K^0 \rightarrow \bar{K}^0$ transition the relevant gluonic corrections are given by the diagrams of Fig. 2. By including gluonic condensate corrections, eq. (3.4) becomes

$$C(Q_{S2}) = -\frac{f^4}{4} \left[1 + \frac{1}{N_c} (1 - \delta_{\langle GG \rangle}) \right], \quad (3.5)$$

where $\delta_{\langle GG \rangle}$ is given by eq. (2.4).

By using the definition given in eq. (1.10) and computing at leading order $\langle \bar{K}^0 | Q_{S2} | K^0 \rangle$, we obtain the following expression for $B_K(\mu)$:

$$B_K(\mu) = \frac{3}{4} \left[1 + \frac{1}{N_c} (1 - \delta_{\langle GG \rangle}) \right] \frac{f^2}{f_K^2}. \quad (3.6)$$

At this stage of the computation, $B_K(\mu)$ does not exhibit yet an explicit dependence on μ . In our approach the scale dependence arises from meson-loop corrections.

If we take $f = f_\pi$ in eq. (3.6) we recover eq. (2.5), as it should be.

Taking $f = f_K$ and $\delta_{\langle GG \rangle} = 0$, eq. (3.6) reproduces the result obtained in the $1/N_c$ approach.

3.2 ONE-LOOP RENORMALIZATION OF THE $\Delta S = 2$ TRANSITION

So far we have ignored chiral-loop corrections to the evaluation of B_K . The introduction of these contributions gives a long-distance μ dependence to $B_K(\mu)$.

In conventional chiral perturbation theory the scale dependence of meson loops renormalization is canceled by construction by the $O(p^4)$ counterterms in the chiral

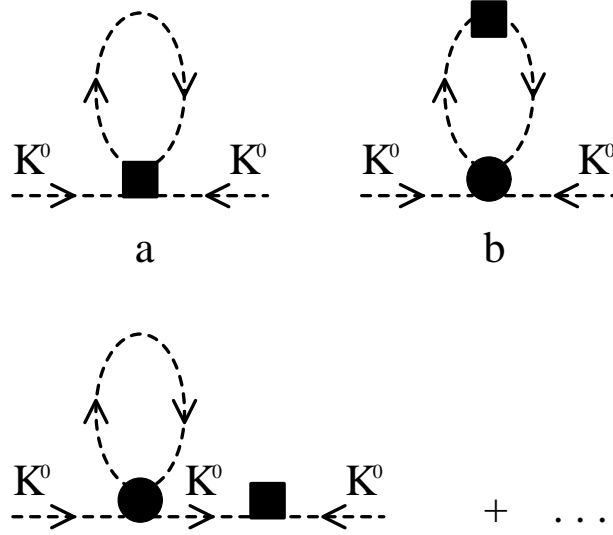


Figure 3: One-loop chiral corrections to the kaon mass matrix. The black box and circle indicate the insertion of the weak $\Delta S = 2$ and strong chiral hamiltonians respectively. The octet mesons K , π , η are exchanged in the loop.

lagrangian. In our approach, on the contrary, the tree-level counterterms are μ independent and the scale dependence introduced in the hadronic matrix elements via the meson loops, evaluated in dimensional regularization with the standard minimal subtraction, is matched with the scale dependence of the Wilson coefficients.

The diagrams relevant to the present case are depicted in Fig. 3. The diagram in Fig. 3(a) contains only a four-meson weak vertex of the $\Delta S = 2$ chiral Lagrangian, while the diagram in Fig. 3(b) contains two vertices, one of which is a four-meson strong vertex and the other is a two-meson weak vertex. Another class of diagrams, which are induced by wave function renormalization, is shown below 3(a,b).

A direct calculation yields:

$$\langle \bar{K}^0 | Q_{S2} | K^0 \rangle_{tree} = C(Q_{S2}) \left(\frac{-4m_K^2}{f^2} \right) \quad (3.7)$$

$$\begin{aligned} \langle \bar{K}^0 | Q_{S2} | K^0 \rangle_{1a} &= i C(Q_{S2}) \frac{1}{f^4} \left[3I_4(m_\eta^2) + I_4(m_\pi^2) + 7m_K^2 I_2(m_\eta^2) \right. \\ &\quad \left. + \frac{7}{3}m_K^2 I_2(m_\pi^2) + \frac{8}{3}m_K^2 [I_2(m_\pi^2) + I_2(m_K^2)] \right] \end{aligned} \quad (3.8)$$

$$\langle \bar{K}^0 | Q_{S2} | K^0 \rangle_{1b} = \frac{4}{3}i C(Q_{S2}) \frac{1}{f^4} [I_4(m_K^2) + 3m_K^2 I_2(m_K^2)]$$

$$+ 3m_K^4 I_3(m_K^2)] \quad (3.9)$$

$$\begin{aligned} \langle \bar{K}^0 | Q_{S2} | K^0 \rangle_{wf} = & -4i C(Q_{S2}) \frac{m_K^2}{f^4} \left[\frac{1}{4} I_2(m_\pi^2) + \frac{1}{4} I_2(m_\eta^2) \right. \\ & \left. + \frac{1}{2} I_2(m_K^2) \right], \end{aligned} \quad (3.10)$$

where $C(Q_{S2})$ is the chiral coefficient given by eq. (3.5), and

$$I_2(m_i^2) = \frac{1}{(2\pi)^4} \int \frac{1}{(q^2 - m_i^2)} d^4q = \frac{i}{(16\pi^2)} m_i^2 \left(1 - \ln \frac{m_i^2}{\mu^2} \right) \quad (3.11)$$

$$I_3(m_i^2) = \frac{1}{(2\pi)^4} \int \frac{1}{(q^2 - m_i^2)^2} d^4q = -\frac{i}{(16\pi^2)} \ln \left(\frac{m_i^2}{\mu^2} \right) \quad (3.12)$$

$$I_4(m_i^2) = \frac{1}{(2\pi)^4} \int \frac{q^2}{(q^2 - m_i^2)} d^4q = \frac{i}{(16\pi^2)} m_i^4 \left(1 - \ln \frac{m_i^2}{\mu^2} \right). \quad (3.13)$$

We also have to consider the meson decay constant renormalization, that is the one-loop determination of f in terms of f_K . This renormalization introduces chiral corrections which cancel some of the contributions coming from meson loops.

Denoting by $\langle \bar{K}^0 | Q_{S2} | K^0 \rangle_{1aNF}$ the non-factorizable chiral corrections coming from the diagrams of Fig. 3(a) that remains after subtracting the kaon decay constant renormalization we have:

$$\begin{aligned} \langle \bar{K}^0 | Q_{S2} | K^0 \rangle_{1aNF} = & 4i C(Q_{S2}) \frac{1}{f^4} \left[-\frac{4}{3} I_4(m_K^2) + \frac{3}{4} I_4(m_\eta^2) + \frac{1}{4} I_4(m_\pi^2) \right. \\ & \left. + \frac{1}{4} m_K^2 [I_2(m_\pi^2) + 3I_2(m_\eta^2)] \right]. \end{aligned} \quad (3.14)$$

The expression for the amplitude, comprehensive of meson loops, wave function and kaon decay constant renormalizations can be written as

$$\begin{aligned} \langle \bar{K}^0 | Q_{S2} | K^0 \rangle = & \langle \bar{K}^0 | Q_{S2} | K^0 \rangle_{tree} + \langle \bar{K}^0 | Q_{S2} | K^0 \rangle_{1b} \\ & + \langle \bar{K}^0 | Q_{S2} | K^0 \rangle_{1aNF}, \end{aligned} \quad (3.15)$$

where the contribution $\langle \bar{K}^0 | Q_{S2} | K^0 \rangle_{tree}$ must be evaluated identifying the chiral lagrangian coefficient f with f_K .

An approach similar to the one that we are adopting here has been followed in ref. [13] in the framework of a cut-off regularization of the chiral loops. It is important to stress that here we have chosen to regularize the divergent integrals appearing in

the meson loops by using dimensional regularization (as we have already done in [20, 2, 3]). This choice is motivated by consistency with the short distance calculation of the Wilson coefficients, which is performed using the same regularization.

In order to show the impact of chiral loops on the K^0 - \bar{K}^0 amplitude, we find convenient to factorize the tree level contribution in terms of the input parameters, while giving the corresponding loop renormalization as a numerical coefficient with an explicit μ dependence. The values of the meson masses and other input variables are those given in Table 2.

We thus find:

$$\langle \bar{K}^0 | Q_{S2} | K^0 \rangle = m_K^2 f_K^2 \left[1 + \frac{1}{N_c} (1 - \delta_{\langle GG \rangle}) \right] (1 + 0.728 + 0.372 \ln \mu^2) . \quad (3.16)$$

From eq. (3.16) we obtain the final result for $B_K(\mu)$, inclusive of the effects of meson loops, wave function and kaon decay constant renormalization:

$$B_K(\mu) = \frac{3}{4} \left[1 + \frac{1}{N_c} (1 - \delta_{\langle GG \rangle}) \right] (1 + 0.728 + 0.372 \ln \mu^2) . \quad (3.17)$$

The scale dependence of the hadronic matrix elements interfere constructively with that of $b(\mu)$. Nevertheless, the overall scale dependence remains below 20% in the range between 0.8 and 1 GeV.

4 NUMERICAL ANALYSIS

We now have all the ingredients necessary to make a detailed analysis of the values of the parameter \hat{B}_K , where $B_K(\mu)$ and $b(\mu)$ are given by eq. (3.17) and eq. (1.5), respectively. The final result depends on the values of the gluon condensate $\langle \alpha_s GG / \pi \rangle$ entering in the determination of the gluon corrections to $B_K(\mu)$ and of $\Lambda_{\text{QCD}}^{(4)}$ which determines the value of the QCD coupling constant α_s , and consequently of $b(\mu)$.

4.1 INPUT PARAMETERS

A relevant input parameter in our present analysis is the gluon condensate. We choose for this quantity the value that gives within a 30% error a fit of the $\Delta I = 3/2$ $K^+ \rightarrow \pi^+ \pi^0$ amplitude:

$$\left\langle \frac{\alpha_s}{\pi} GG \right\rangle = (360 \pm 15 \text{ MeV})^4 . \quad (4.1)$$

parameter	value
$f_\pi = f_{\pi^+}$	92.4 MeV
$f_K = f_{K^+}$	113 MeV
$m_\pi = (m_{\pi^+} + m_{\pi^0})/2$	138 MeV
$m_K = m_{K^0}$	498 MeV
m_η	548 MeV
$\Lambda_{\text{QCD}}^{(4)}$	350 ± 100 MeV

Table 2: Table of the numerical values used for the input parameters.

Our results depend very little on the quark condensate that we keep fixed at the value $\langle \bar{q}q \rangle = - (280 \text{ MeV})^3$, which gives the best fit of the $\Delta I = 1/2$ $K^0 \rightarrow \pi\pi$ amplitude.

A word of caution concerning the renormalization prescription of the chiral lagrangian parameter f in the amplitudes: in refs. [20, 2, 3] we have included the one-loop renormalization of $1/f^3$ in the $K \rightarrow \pi\pi$ tree level chiral amplitudes. From now on we include in the counting of powers of f also the f dependence of the chiral coefficient computed in the χ QM. For the $K \rightarrow \pi\pi$ amplitudes it amounts to replace $1/f^3 \rightarrow f$. The numerical consequence of this change in prescription is that the best fit of the $\Delta I = 1/2$ rule leads to a central value of the gluon condensate $\langle \alpha_s GG/\pi \rangle = (360 \text{ MeV})^4$, slightly smaller than that obtained in [2], namely $(372 \text{ MeV})^4$.

Another input parameter which is important for the determination of \hat{B}_K , is the QCD running coupling constant α_s entering in the computation of the short distance factor $b(\mu)$. In our numerical estimates we use for α_s the range of eq.(1.8), corresponding to the values of $\Lambda_{\text{QCD}}^{(4)}$ given by (1.9). The values of this and other input parameters are listed in Table 2.

4.2 NUMERICAL RESULTS FOR \hat{B}_K

Our numerical estimate of the parameter \hat{B}_K is summarized in Table 3, in which we have fixed $\langle \alpha_s GG/\pi \rangle$ to the central value of eq. (4.1) and we have examined two extreme values of the matching scale μ in both schemes HV and NDR. The three parts of the table show the dependence on the QCD scale parameter $\Lambda_{\text{QCD}}^{(4)}$.

From Table 3 we obtain the ranges $0.79 \leq \hat{B}_K \leq 1.0$ in NDR and $0.69 \leq \hat{B}_K \leq 0.97$ in HV scheme.

The quantities $\Delta_{\gamma_5} \hat{B}_K$ and $\Delta_\mu \hat{B}_K$ measure the size of the γ_5 -scheme and μ -dependences respectively,

$$\Delta_{\gamma_5} \hat{B}_K = 2 \left| \frac{\hat{B}_K|_{\text{HV}} - \hat{B}_K|_{\text{NDR}}}{\hat{B}_K|_{\text{HV}} + \hat{B}_K|_{\text{NDR}}} \right| \quad (4.2)$$

$$\Delta_\mu \hat{B}_K = 2 \left| \frac{\hat{B}_K(1 \text{ GeV}) - \hat{B}_K(0.8 \text{ GeV})}{\hat{B}_K(1 \text{ GeV}) + \hat{B}_K(0.8 \text{ GeV})} \right|. \quad (4.3)$$

The scale dependence $\Delta_\mu \hat{B}_K$ is near to 20% in both schemes and it is mainly due to the effect of meson loops renormalization. As a matter of fact the final μ dependence is larger than the one originally present in the coefficient $b(\mu)$, which is less than 10%. Nevertheless the fact that the scale dependence is at most 20% makes us confident on the stability of our results. and allows us to choose $\mu = 0.8 \text{ GeV}$ as the best compromise between the upper limit of validity of chiral perturbation theory, used to compute $B_K(\mu)$, and the lowest scale for perturbative calculations, needed to obtain the short distance coefficient $b(\mu)$.

The scheme dependence of our result is entirely due to $b(\mu)$, since the hadronic matrix element does not exhibit any scheme dependence. At any rate $\Delta_{\gamma_5} \hat{B}_K$ is below 10% for all values of μ in the given range.

Finally, a few words on the dependence of our results on the value chosen for the gluon condensate. In Fig. 4 we show \hat{B}_K as a function of the gluon condensate, for our preferred matching scale $\mu = 0.8 \text{ GeV}$, and $\Lambda_{\text{QCD}}^{(4)} = 350 \text{ MeV}$.

It appears that \hat{B}_K is a sensitive decreasing function of the gluon condensate. For our values of $\langle \alpha_s GG/\pi \rangle$ the term $\delta_{\langle GG \rangle}$ in eq. (3.17) is greater than 1, thus changing the sign of the $1/N_c$ contribution and determining a reduction of the final result for \hat{B}_K . By varying also the value of the gluon condensate in the range of eq. (4.1) we obtain the overall range

$$0.54 \leq \hat{B}_K \leq 1.2. \quad (4.4)$$

which represents our conservative prediction for B_K . The central value $\hat{B}_K = 0.87$, quoted in the abstract, is obtained by taking all input parameters at their central values. It represents a large renormalization with respect to the initial value given by eq. (2.5). In this respect, improving to $O(p^4)$ the chiral expansion, albeit challenging, might be needed in order to assess the degree of stability of the result.

$\Lambda_{\text{QCD}}^{(4)} = 250 \text{ MeV}$				
	$\mu = 0.8 \text{ GeV}$		$\mu = 1 \text{ GeV}$	
	NDR	HV	NDR	HV
$b(\mu)$	1.25	1.19	1.30	1.24
\widehat{B}_K	0.88	0.84	1.01	0.97
$\Delta_{\gamma_5} \widehat{B}_K$	5.2%		4.2%	
$\Delta_\mu \widehat{B}_K$	14% – 15%			
$\Delta_\mu b(\mu)$	4% – 5%			
$\Lambda_{\text{QCD}}^{(4)} = 350 \text{ MeV}$				
	$\mu = 0.8 \text{ GeV}$		$\mu = 1 \text{ GeV}$	
	NDR	HV	NDR	HV
$b(\mu)$	1.17	1.08	1.23	1.17
\widehat{B}_K	0.83	0.77	0.96	0.91
$\Delta_{\gamma_5} \widehat{B}_K$	8%		5.7%	
$\Delta_\mu \widehat{B}_K$	15% – 17%			
$\Delta_\mu b(\mu)$	5% – 7%			
$\Lambda_{\text{QCD}}^{(4)} = 450 \text{ MeV}$				
	$\mu = 0.8 \text{ GeV}$		$\mu = 1 \text{ GeV}$	
	NDR	HV	NDR	HV
$b(\mu)$	1.12	0.97	1.18	1.09
\widehat{B}_K	0.79	0.69	0.92	0.85
$\Delta_{\gamma_5} \widehat{B}_K$	14.1%		7.9%	
$\Delta_\mu \widehat{B}_K$	15% – 21%			
$\Delta_\mu b(\mu)$	5% – 11%			

Table 3: Matching scale and γ_5 scheme dependence of \hat{B}_K in the χ QM with NLO Wilson coefficients, for various values of $\Lambda_{\text{QCD}}^{(4)}$. We take for the gluon condensate the value $\langle \alpha_s GG/\pi \rangle = (360 \text{ MeV})^4$, preferred by the fit of $\Gamma(K^+ \rightarrow \pi^+ \pi^0)$.

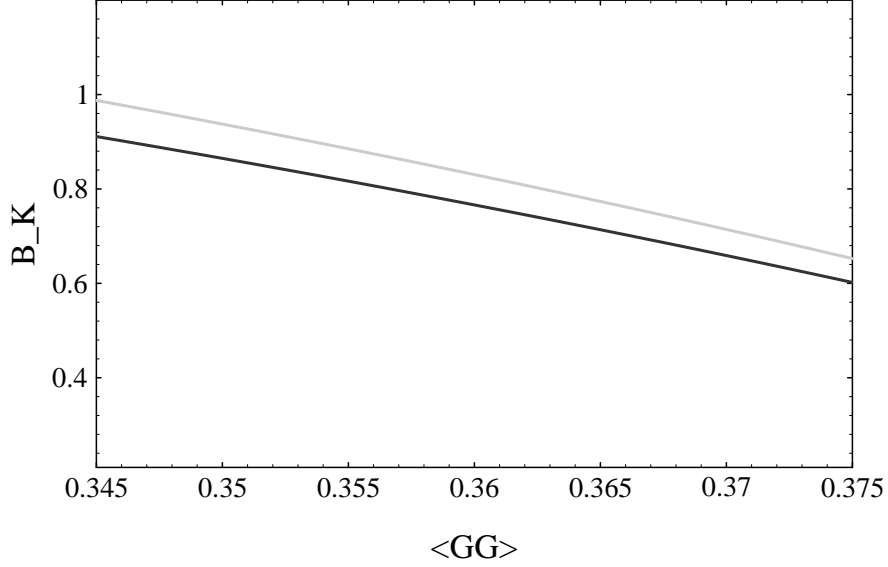


Figure 4: The \hat{B}_K parameter is shown as a function of the gluon condensate for $\Lambda_{\text{QCD}}^{(4)} = 350$ MeV and $\mu = 0.8$ GeV. We denote by $\langle GG \rangle$ the quantity $\langle \alpha_s GG / \pi \rangle^{1/4}$ in units of GeV. The dark and grey lines represent the HV and NDR results respectively.

5 K_L - K_S MASS DIFFERENCE

We apply the results of the previous section to the study of the K_L^0 - K_S^0 mass difference ΔM_{LS} . The full ΔM_{LS} can be split into short- and long-distance components as

$$\Delta M_{LS} = \Delta M_{SD} + \Delta M_{LD}. \quad (5.1)$$

Notice that the “short-distance” component ΔM_{SD} , generated by the lagrangian in eq. (1.1), contains the hadronic parameter \hat{B}_K . The value of \hat{B}_K estimated in the previous part of the paper completes the determination of the box (or short-distance) component of ΔM_{LS} .

We address now the issue of the evaluation of the genuine long-distance contribution ΔM_{LD} . We will do it consistently with the evaluation of B_K . The interesting question is whether the interplay between ΔM_{SD} and ΔM_{LD} reproduces the observed value $\Delta M_{LS}^{\text{exp}}$.

5.1 LONG DISTANCE $\Delta S = 1$ INDUCED CONTRIBUTIONS

Many attempts have been made to estimate ΔM_{LD} [26]–[33] by means of various techniques like chiral symmetry, dispersion relation with experimental data of s -wave $\pi\pi$ scattering, leading to a variety of numerical results.

Our aim is to give a consistent estimate of ΔM_{LD} based on the χ QM approach.

As already mentioned, the K^0 - \bar{K}^0 mass difference receives contributions from the exchange of the $SU(3)$ meson field octet (we leave aside in this analysis the contribution of η') via the double insertion of the $\Delta S = 1$ chiral vertices.

The complete bosonization of the $\Delta S = 1$ lagrangian of eq. (1.21) can be found in ref. [34]. Here we just quote the result for the operators Q_{1-6} , which turn out to be relevant for the calculation of ΔM_{LD} . The electroweak penguins Q_{7-10} give a negligible contribution (of the order of 1%) due the smallness of their Wilson coefficients.

The bosonization of the relevant operators leads to

$$\begin{aligned} \mathcal{L}_{\Delta S=1}^{(2)} = & G_{\underline{8}}(Q_{3-6}) \text{Tr} \left(\lambda_2^3 D_\mu \Sigma^\dagger D^\mu \Sigma \right) + \\ & G_{LL}^a(Q_{1,2}) \text{Tr} \left(\lambda_1^3 \Sigma^\dagger D_\mu \Sigma \right) \text{Tr} \left(\lambda_2^1 \Sigma^\dagger D^\mu \Sigma \right) + \\ & G_{LL}^b(Q_{1,2}) \text{Tr} \left(\lambda_2^3 \Sigma^\dagger D_\mu \Sigma \right) \text{Tr} \left(\lambda_1^1 \Sigma^\dagger D^\mu \Sigma \right), \end{aligned} \quad (5.2)$$

where, as before, λ_j^i are combinations of Gell-Mann $SU(3)$ matrices defined by $(\lambda_j^i)_{lk} = \delta_{il}\delta_{jk}$ and Σ is defined in eq. (3.2). The covariant derivatives in eq. (5.2) are taken with respect to the external gauge fields whenever they are present.

The notation for the chiral coefficients $G_{\underline{8}}(Q_{3-6})$, $G_{LL}^a(Q_{1,2})$ and $G_{LL}^b(Q_{1,2})$ reminds us their chiral properties: $G_{\underline{8}}$ represents the $(\underline{8}_L \times \underline{1}_R)$ part of the interaction induced in QCD by the gluonic penguins, while the two terms proportional to G_{LL}^a and G_{LL}^b are admixtures of the $(\underline{27}_L \times \underline{1}_R)$ and the $(\underline{8}_L \times \underline{1}_R)$ part of the interaction, induced by left-handed current-current operators. These coefficient have been evaluated in two different schemes of regularization HV and NDR, and the results are given in Table 4. In this table M is the constituent quark mass, that, consistently with previous analyses, we take at 220 MeV and Λ_χ is the chiral symmetry breaking scale ($\simeq 1$ GeV).

The diagrams relevant to the evaluation of the long-distance contribution ΔM_{LD} arise via one-particle and two-particle intermediate states (three-particle intermediate states have been shown not to give significant contributions [28]). They contain

HV	NDR
$G_{LL}^a(Q_1) = -\frac{1}{N_c} f_\pi^4 (1 - \delta_{\langle GG \rangle})$	$G_{LL}^a(Q_1) = -\frac{1}{N_c} f_\pi^4 (1 - \delta_{\langle GG \rangle})$
$G_{LL}^a(Q_2) = -f_\pi^4$	$G_{LL}^a(Q_2) = -f_\pi^4$
$G_{LL}^b(Q_1) = -f_\pi^4$	$G_{LL}^b(Q_1) = -f_\pi^4$
$G_{LL}^b(Q_2) = -\frac{1}{N_c} f_\pi^4 (1 - \delta_{\langle GG \rangle})$	$G_{LL}^b(Q_2) = -\frac{1}{N_c} f_\pi^4 (1 - \delta_{\langle GG \rangle})$
$G_{\underline{8}}(Q_3) = f_\pi^4 \frac{1}{N_c} (1 - \delta_{\langle GG \rangle})$	$G_{\underline{8}}(Q_3) = f_\pi^4 \frac{1}{N_c} (1 - \delta_{\langle GG \rangle} - 6 \frac{M^2}{\Lambda_\chi^2})$
$G_{\underline{8}}(Q_4) = f_\pi^4$	$G_{\underline{8}}(Q_4) = f_\pi^4 (1 - 6 \frac{M^2}{\Lambda_\chi^2})$
$G_{\underline{8}}(Q_5) = \frac{2}{N_c} \frac{\langle \bar{q}q \rangle}{M} f_\pi^2 (1 - 6 \frac{M^2}{\Lambda_\chi^2})$	$G_{\underline{8}}(Q_5) = \frac{2}{N_c} \frac{\langle \bar{q}q \rangle}{M} f_\pi^2 (1 - 9 \frac{M^2}{\Lambda_\chi^2})$
$G_{\underline{8}}(Q_6) = 2 \frac{\langle \bar{q}q \rangle}{M} f_\pi^2 (1 - 6 \frac{M^2}{\Lambda_\chi^2})$	$G_{\underline{8}}(Q_6) = 2 \frac{\langle \bar{q}q \rangle}{M} f_\pi^2 (1 - 9 \frac{M^2}{\Lambda_\chi^2})$

Table 4: Values of the relevant $\Delta S = 1$ weak chiral coefficients for two different regularization schemes: HV and NDR. The inclusion of the Wilson coefficients of the effective quark operators Q_i is understood.

two weak vertices, among those proportional to $G_{\underline{8}}$, G_{LL}^a and G_{LL}^b . Therefore we have to consider all the possible combinations: $G_{LL}^a G_{LL}^a$, $G_{LL}^b G_{LL}^b$, $G_{\underline{8}} G_{\underline{8}}$, $G_{LL}^a G_{LL}^b$, $G_{\underline{8}} G_{LL}^a$, $G_{\underline{8}} G_{LL}^b$.

Using the Feynman rules reported in appendix A, it is found that the single particle intermediate state contribution give a result proportional to $(4m_K^2 - m_\pi^2 - 3m_\eta^2)$ which vanishes [26] by the Gell-Mann-Okubo relation.

A non-vanishing contribution is obtained from the two particle intermediate states, which corresponds to the double insertion of the $\Delta S = 1$ chiral lagrangian as depicted in Fig. 5(a) and 5(b). To our knowledge, the relevance of the diagrams of the type (b) (tadpole diagrams) was first pointed out in ref. [32].

The calculation is lengthy and the details can be found in refs. [36]. In evaluating the loop integrals, we use dimensional regularization and modified minimal subtraction.

5.2 $\Delta S = 1$ WILSON COEFFICIENTS

In Table 5 we report the Wilson coefficients of the first six operators at the scale $\mu = 0.8$ GeV in the NDR and HV γ_5 -schemes, respectively. Since $\text{Re } \tau$ in eq. (1.21)

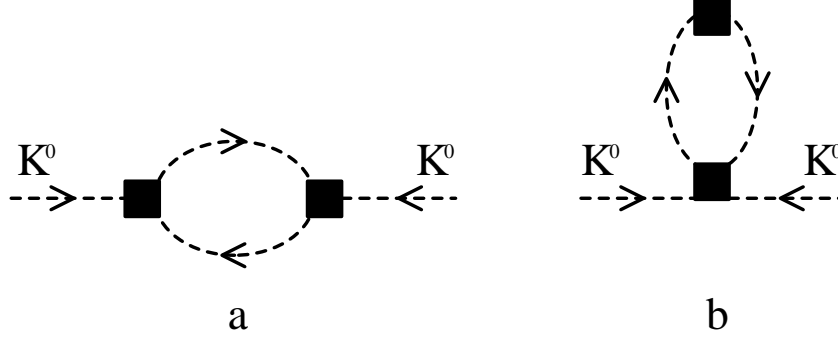


Figure 5: One-loop long-distance contributions to the $K^0 - \bar{K}^0$ mixing induced by the $\Delta S = 1$ weak hamiltonian. The black box represents the insertion of the $\Delta S = 1$ chiral interactions. The octet mesons K , π , η are exchanged in the loop.

is of $O(10^{-3})$, the $K^0 \leftrightarrow \bar{K}^0$ transition is controlled by the coefficients z_i , which do not depend on m_t .

5.3 $\Delta S = 2$ WILSON COEFFICIENTS

The Wilson coefficients of the $\Delta S = 2$ effective quark operator are denoted by η_1 , η_2 and η_3 (see eq. (1.1)).

The NLO calculations of η_1 and η_2 can be found in refs. [6] and [5] respectively, while the analogous calculation for η_3 , which is particularly challenging, has been performed only recently by the authors of ref. [7]. We have taken their results and evaluated the QCD factors for our choice of parameters.

As an example, for $\Lambda_{\text{QCD}}^{(4)} = 350$ MeV and $m_t^{(pole)} = 180$ GeV, at the scale $\mu = m_c = 1.4$ GeV we find

$$\eta_1 = 1.36 \quad \eta_2 = 0.51 \quad \eta_3 = 0.45 \quad (5.3)$$

5.4 NUMERICAL ANALYSIS

According to Wolfenstein's notation [35], we define the parameter D which characterizes the long distance contribution

$$D = \frac{\Delta M_{LD}}{\Delta M_{LS}^{exp}}. \quad (5.4)$$

Numerical estimates of D , ΔM_{LD} and ΔM_{SD} for different values of $\Lambda_{\text{QCD}}^{(4)}$ and of the matching scale μ are given in Table 6. In this table we have fixed the gluon

$\Lambda_{QCD}^{(4)}$	250 MeV		350 MeV		450 MeV	
$\alpha_s(m_Z)_{\overline{MS}}$	0.113		0.119		0.125	
NDR						
z_1	(0.0503)	−0.524	(0.0533)	−0.663	(0.0557)	−0.781
z_2	(0.982)	1.29	(0.981)	1.39	(0.980)	1.48
z_3		0.0180		0.0360		0.0870
z_4		−0.0471		−0.0852		−0.182
z_5		0.0085		0.0077		−0.0129
z_6		−0.0495		−0.0947		−0.226
HV						
z_1	(0.0320)	−0.657	(0.0339)	−0.910	(0.0355)	−1.36
z_2	(0.988)	1.38	(0.987)	1.58	(0.987)	1.96
z_3		0.0137		0.0301		0.0798
z_4		−0.0292		−0.0540		−0.115
z_5		0.0070		0.0100		0.0123
z_6		−0.0275		−0.0515		−0.112

Table 5: NLO Wilson coefficients at $\mu = 0.8$ GeV in the NDR and in the HV scheme ($\alpha = 1/128$). The corresponding values at $\mu = m_W$ are given in parenthesis. In addition one has $z_{3-6}(m_c) = 0$. The coefficients $z_i(\mu)$ do not depend on m_t .

$\Lambda_{\text{QCD}}^{(4)} = 250 \text{ MeV}$				
	$\mu = 0.8 \text{ GeV}$		$\mu = 1 \text{ GeV}$	
	NDR	HV	NDR	HV
ΔM_{SD}	2.55	2.42	2.92	2.80
ΔM_{LD}	-0.34	-0.38	-0.35	-0.38
D	-0.10	-0.11	-0.10	-0.11
$\Delta M^{th}/\Delta M^{exp}$	0.63	0.58	0.73	0.69
$\Lambda_{\text{QCD}}^{(4)} = 350 \text{ MeV}$				
	$\mu = 0.8 \text{ GeV}$		$\mu = 1 \text{ GeV}$	
	NDR	HV	NDR	HV
ΔM_{SD}	3.07	2.83	3.56	3.37
ΔM_{LD}	-0.54	-0.65	-0.46	-0.51
D	-0.15	-0.18	-0.13	-0.14
$\Delta M^{th}/\Delta M^{exp}$	0.72	0.62	0.88	0.81
$\Lambda_{\text{QCD}}^{(4)} = 450 \text{ MeV}$				
	$\mu = 0.8 \text{ GeV}$		$\mu = 1 \text{ GeV}$	
	NDR	HV	NDR	HV
ΔM_{SD}	3.91	3.40	4.55	4.20
ΔM_{LD}	-1.18	-1.50	-0.65	-0.75
D	-0.34	-0.43	-0.18	-0.21
$\Delta M^{th}/\Delta M^{exp}$	0.77	0.54	1.11	0.98

Table 6: Long-distance and short-distance box contributions to ΔM_{LS} , in units of 10^{-15} GeV , for different values of the matching scale μ and $\Lambda_{\text{QCD}}^{(4)}$ in the χQM . We take for the gluon condensate the value $\langle\alpha_s GG/\pi\rangle = (360 \text{ MeV})^4$ and for the quark condensate $\langle\bar{q}q\rangle = -(280 \text{ MeV})^3$, which are the values preferred by the fit of the $\Delta I = 1/2$ selection rule at the same perturbative order. The “short-distance” component ΔM_{SD} is evaluated for a top quark pole mass of 180 GeV and for the values of \hat{B}_K given in Table 3.

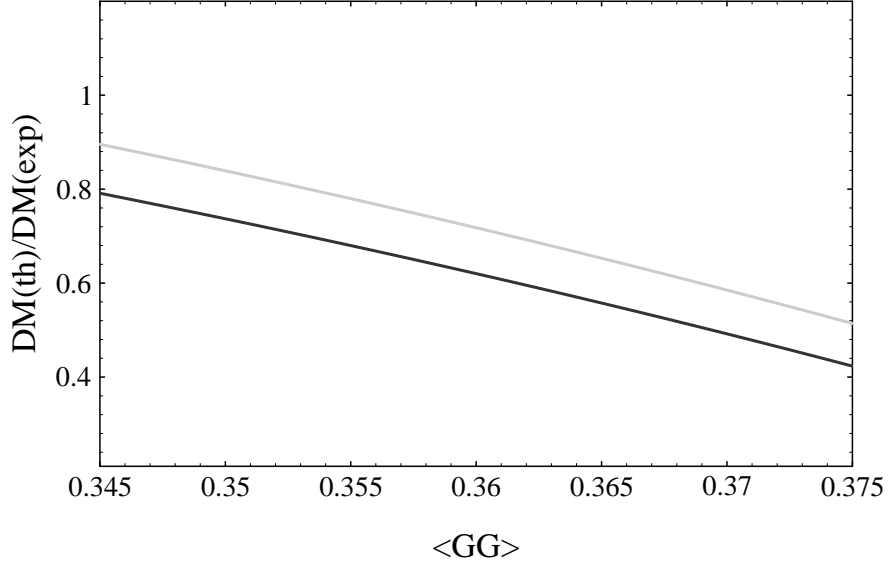


Figure 6: The ratio $(\Delta M_{SD} + \Delta M_{LD})/\Delta M_{LS}^{exp}$ is shown as a function of the gluon condensate for $\Lambda_{QCD}^{(4)} = 350$ MeV and $\mu = 0.8$ GeV. We denote by $\langle GG \rangle$ the quantity $\langle \alpha_s GG/\pi \rangle^{1/4}$ in units of GeV. The dark and grey lines represent the HV and NDR results respectively.

condensate to our central value $\langle \alpha_s GG/\pi \rangle = (360 \text{ MeV})^4$ and we have chosen for the quark condensate the value $\langle \bar{q}q \rangle = -(280 \text{ MeV})^3$ which gives us the best fit of the $\Delta I = 1/2$ selection rule. The ranges thus obtained are $0.63 \leq \Delta M_{LS}^{th}/\Delta M_{LS}^{exp} \leq 1.11$ in the NDR and $0.54 \leq \Delta M_{LS}^{th}/\Delta M_{LS}^{exp} \leq 0.98$ in the HV.

A few comments are in order. Among the diagrams of Fig. 5(a), those containing two intermediate pion states dominate over kaon and eta exchange by about a factor of two. The diagrams of Fig. 5(b) (tadpole diagrams) give a contribution comparable in size with those of Fig. 5(a) but of the opposite sign, leading to a small and negative ΔM_{LD} in most of the parameter space.

We disagree with ref. [32] in the details of the calculation and on the the relevant interactions. In particular, the author of ref. [32] seems to neglect some of the leading insertions of the operator Q_2 , according to our computation.

Our result depends on the value of the gluon condensate. Fig. 6 shows the typical behavior for a choice of input parameters. The total theoretical mass difference ΔM_{LS}^{th} is a decreasing function of the value of the gluon condensate, analogously to

the case of \hat{B}_K . If we let the value of the gluon condensate vary in the range of eq. (4.1), as we did in determining \hat{B}_K , we obtain the overall range

$$0.42 \leq \Delta M_{LS}^{th}/\Delta M_{LS}^{exp} \leq 1.40 \quad (5.5)$$

which represents our most conservative result.

The scheme dependence of the result is satisfactory ($< 20\%$) for most of the range of $\Lambda_{\text{QCD}}^{(4)}$. Less satisfactory is the renormalization scale dependence. ΔM_{SD} is an increasing function of μ and this behavior is not compensated by a corresponding decrease of the D parameter. This feature leads to a scale dependence that is about 30% for $\Lambda_{\text{QCD}}^{(4)} \leq 350$ MeV. These results may indicate the need to extend the analysis to $O(p^4)$ in the chiral lagrangian expansion. An improved χQM calculation of the $\Delta S = 1$ and $\Delta S = 2$ chiral coefficients at $O(p^4)$ is under way.

A final comment about the width difference $\Delta\Gamma_{LS}$ is necessary. A direct calculation of the absorptive component of Fig. 5(a) gives about 1/6 of the experimental result. The reason is that the tree-level $K \rightarrow \pi\pi$ decay amplitudes do not reproduce the measured ones. Only by replacing in the vertices of Fig. 5(a) the one-loop results obtained in [2], we obtain the agreement with the experimental $\Delta\Gamma_{LS}$. This is equivalent to computing directly the absorptive part of Fig. 5(a) up to three loops.

6 THE MIXING PARAMETER $\text{Im } \lambda_t$

A range for the KM parameter $\text{Im } \lambda_t$, which is relevant for CP violating observables, can be determined from the experimental value of ε as a function of \hat{B}_K , m_t and the other relevant parameters involved in the theoretical estimate.

Given m_t , m_c and the KM parameters [23]

$$|V_{us}| = 0.2205 \pm 0.0018 \quad (6.1)$$

$$|V_{cb}| = 0.041 \pm 0.003 \quad (6.2)$$

$$|V_{ub}/V_{cb}| = 0.08 \pm 0.02, \quad (6.3)$$

we can solve the two equations

$$\varepsilon^{th}(\hat{B}_K, |V_{cb}|, |V_{us}|, \Lambda_{\text{QCD}}^{(4)}, m_t, m_c, \eta, \rho) = \varepsilon^{exp} \quad (6.4)$$

$$\eta^2 + \rho^2 = \frac{1}{|V_{us}|^2} \left| \frac{V_{ub}}{V_{cb}} \right|^2 \quad (6.5)$$

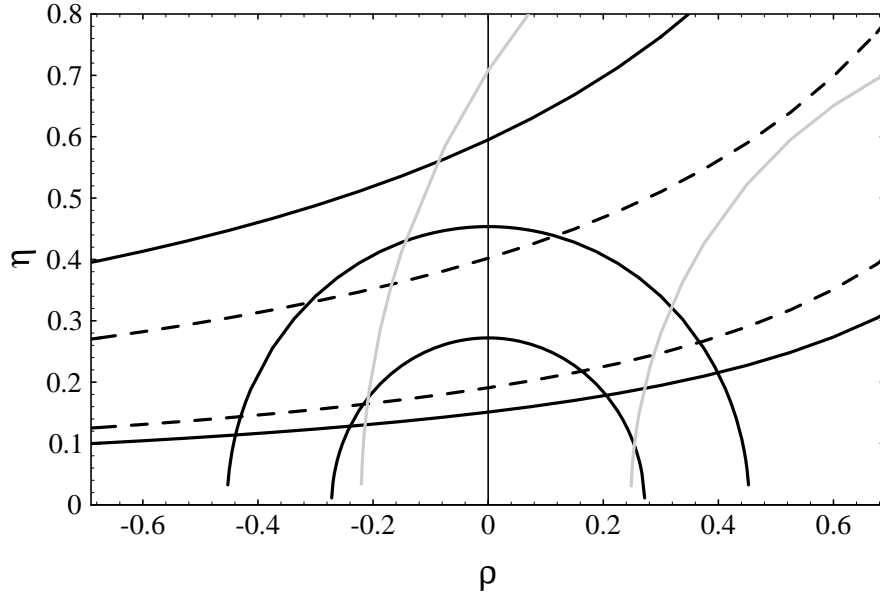


Figure 7: Constraints on KM parameters from kaon physics. See the text for explanation.

to find the allowed values of the two parameters η and ρ appearing in the Wolfenstein parametrization of KM mixing matrix.

We include in this analysis the interval of values for $\Lambda_{\text{QCD}}^{(4)}$ in eq. (1.9) and for the gluon condensate the range in eq. (4.1). The matching scale μ is varied between 0.8 and 1 GeV, while \hat{B}_K is varied according to the range obtained in the previous sections. The results for $m_t^{(pole)} = 180$ GeV are presented graphically in Fig. 7.

We can see that the equations (6.4) and (6.5) define two families of curves (respectively hyperbola and circles) in the $(\rho-\eta)$ plane. The allowed values of the two parameters correspond to the region delimited by the intersections between the two families of curves. The area enclosed by the two solid line hyperbolae corresponds to our most conservative range $0.54 < \hat{B}_K < 1.2$.

This procedure gives two possible ranges for η and consequently for $\text{Im } \lambda_t \simeq \eta |V_{us}| |V_{cb}|^2$, which correspond to having the KM phase in the I or II quadrant (ρ positive or negative, respectively). For the central value of the top mass ($\bar{m}_t(m_W) \simeq 183$ GeV) we find

$$0.67 \times 10^{-4} \leq \text{Im } \lambda_t \leq 1.7 \times 10^{-4} \quad (6.6)$$

in the first quadrant and

$$0.41 \times 10^{-4} \leq \text{Im } \lambda_t \leq 1.7 \times 10^{-4} \quad (6.7)$$

in the second quadrant.

We also consider a “biased” estimate of $\text{Im } \lambda_t$, obtained by fixing the gluon condensate and $\Lambda_{\text{QCD}}^{(4)}$ to their central values and varying the matching scale μ between 0.8 and 1 GeV. In this way we are spanning the following range for the renormalization group invariant parameter \hat{B}_K :

$$\hat{B}_K = 0.87 \pm 0.10, \quad (6.8)$$

This choice of the input parameters restricts the hyperbolic band to the area enclosed by the dashed lines in Fig. 7. The overlap with the constraint of eq. (6.5) leads to the following ranges of allowed values for $\text{Im } \lambda_t$

$$0.81 \times 10^{-4} \leq \text{Im } \lambda_t \leq 1.6 \times 10^{-4} \quad (6.9)$$

in the first quadrant and

$$0.52 \times 10^{-4} \leq \text{Im } \lambda_t \leq 1.5 \times 10^{-4} \quad (6.10)$$

in the second quadrant.

Varying m_t in the range $m_t^{(pole)} = 180 \pm 12$ GeV affects very little the quoted lower bounds on $\text{Im } \lambda_t$ while the upper bounds are changed by less than 20% (decreasing m_t corresponds to increasing the upper limits). On the other hand, the upper bound on $\text{Im } \lambda_t$ remains stable, being bounded by the maximum value of η obtained from eq. (6.5) ($\rho = 0$).

We do not discuss here details of the bounds provided by ΔM_{B_d} which are represented, for the central value of m_t , by the area delimited by the grey lines in Fig. 7. The constraints of $B_d - \bar{B}_d$ mixing have a marginal impact in the determination of the overall range of η . As the example in the figure shows, only the lower bound of $\text{Im } \lambda_t$ in the second quadrant is affected by such an inclusion and raised to 0.6×10^{-4} .

A FEYNMAN RULES FOR THE $\Delta S = 1$ CHIRAL LAGRANGIAN

We report the Feynman rules for the three terms (proportional to G_{LL}^a , G_{LL}^b and G_8) of the $\Delta S = 1$ chiral lagrangian which are relevant for the calculation of the long-distance contribution ΔM_{LD} . All momenta are entering the vertex.

G_{LL}^a :

$$\begin{aligned}
K^+(p_1)\pi^-(p_2) & \quad \frac{2i}{f^2} p_1 \cdot p_2 \\
K^0(p_1)\pi^+(p_2)\pi^-(p_3) & \quad -\frac{\sqrt{2}}{f^3} p_3 \cdot (p_2 - p_1) \\
K^0(p_1)K^+(p_2)K^-(p_3) & \quad -\frac{\sqrt{2}}{f^3} p_2 \cdot (p_1 - p_3) \\
K^0(p_1)K^0(p_2)\pi^+(p_3)K^-(p_4) & \quad \frac{i}{f^4} \left[p_1 \cdot p_2 - \left(\frac{p_1 + p_2}{2} \right) \cdot (p_3 + p_4) + p_3 \cdot p_4 \right]
\end{aligned} \tag{A.1}$$

G_{LL}^b :

$$\begin{aligned}
K^0(p_1)\pi^0(p_2) & \quad \frac{i\sqrt{2}}{f^2} p_1 \cdot p_2 \\
K^0(p_1)\eta(p_2) & \quad \frac{i}{f^2} \sqrt{\frac{2}{3}} p_1 \cdot p_2 \\
K^0(p_1)\pi^0(p_2)\pi^0(p_3) & \quad -\frac{1}{\sqrt{2}f^3} \left[p_1 \cdot \left(\frac{p_2 + p_3}{2} \right) - p_2 \cdot p_3 \right] \\
K^0(p_1)\eta(p_2)\eta(p_3) & \quad -\frac{1}{\sqrt{2}f^3} \left[p_2 \cdot p_3 - p_1 \cdot \left(\frac{p_2 + p_3}{2} \right) \right] \\
K^0(p_1)K^+(p_2)K^-(p_3) & \quad -\frac{\sqrt{2}}{f^3} (-p_1 \cdot p_3 + p_1 \cdot p_2) \\
K^0(p_1)\pi^+(p_2)\pi^-(p_3) & \quad -\frac{\sqrt{2}}{f^3} (-p_1 \cdot p_3 + p_1 \cdot p_2) \\
K^0(p_1)\eta(p_2)\pi^0(p_3) & \quad -\frac{1}{\sqrt{6}f^3} (p_1 \cdot p_2 + 2p_2 \cdot p_3 - 3p_1 \cdot p_3) \\
K^0(p_1)K^0(p_2)\bar{K}^0(p_3)\pi^0(p_4) & \quad \frac{2\sqrt{2}}{3} \frac{i}{f^4} \left[p_3 \cdot p_4 - \left(\frac{p_1 + p_2}{2} \right) \cdot p_4 \right] \\
K^0(p_1)K^0(p_2)\pi^+(p_3)K^-(p_4) & \quad \frac{i}{3f^4} \left[4p_1 \cdot p_2 - 2 \left(\frac{p_1 + p_2}{2} \right) \cdot (p_4 + p_3) \right]
\end{aligned} \tag{A.2}$$

$$K^0(p_1)K^0(p_2)\bar{K}^0(p_3)\eta(p_4) \quad \frac{2}{3}\sqrt{\frac{2}{3}}\frac{i}{f^4}\left[p_3 \cdot p_4 - \left(\frac{p_1 + p_2}{2}\right) \cdot p_4\right]$$

$G_{\underline{8}}$:

$$\begin{aligned}
K^0(p_1)\pi^0(p_2) & \quad \frac{i\sqrt{2}}{f^2} p_1 \cdot p_2 \\
K^0(p_1)\eta(p_2) & \quad \frac{i}{f^2}\sqrt{\frac{2}{3}} p_1 \cdot p_2 \\
K^+(p_1)\pi^-(p_2) & \quad -\frac{2i}{f^2} p_1 \cdot p_2 \\
K^0(p_1)\pi^0(p_2)\pi^0(p_3) & \quad -\frac{1}{2\sqrt{2}f^3} [p_3 \cdot (p_1 - p_2) + p_2 \cdot (p_1 - p_3)] \\
K^0(p_1)\pi^0(p_2)\eta(p_3) & \quad -\frac{1}{\sqrt{6}f^3} (p_1 \cdot p_3 + 2p_2 \cdot p_3 - 3p_1 \cdot p_2) \\
K^0(p_1)\eta(p_2)\eta(p_3) & \quad -\frac{1}{\sqrt{2}f^3} \left[p_2 \cdot p_3 - p_1 \cdot \left(\frac{p_2 + p_3}{2} \right) \right] \\
K^0(p_1)K^+(p_2)K^-(p_3) & \quad -\frac{\sqrt{2}}{f^3} p_3 \cdot (p_2 - p_1) \\
K^0(p_1)\pi^+(p_2)\pi^-(p_3) & \quad -\frac{\sqrt{2}}{f^3} p_2 \cdot (p_1 - p_3) \\
K^0(p_1)K^0(p_2)\bar{K}^0(p_3)\pi^0(p_4) & \quad \frac{2\sqrt{2}}{3}\frac{i}{f^4} \left[p_3 \cdot p_4 - \left(\frac{p_1 + p_2}{2} \right) \cdot p_4 \right] \\
K^0(p_1)K^0(p_2)\pi^+(p_3)K^-(p_4) & \quad \frac{i}{3f^4} \left[p_1 \cdot p_2 + (p_4 + p_3) \left(\frac{p_1 + p_2}{2} \right) - 3p_3 \cdot p_4 \right] \\
K^0(p_1)K^0(p_2)\bar{K}^0(p_3)\eta(p_4) & \quad \frac{2}{3}\sqrt{\frac{2}{3}}\frac{i}{f^4} \left[p_3 \cdot p_4 - \left(\frac{p_1 + p_2}{2} \right) \cdot p_4 \right]
\end{aligned} \tag{A.3}$$

REFERENCES

- [1] K. Nishijima, *Nuovo Cim.* **11** (1959) 698;
 F. Gursey, *Nuovo Cim.* **16** (1960) 230 and *Ann. Phys. (NY)* **12** (1961) 91;
 J.A. Cronin, *Phys. Rev.* **161** (1967) 1483;
 S. Weinberg, *Physica* **96A** (1979) 327;
 A. Manohar and H. Georgi, *Nucl. Phys.* **B 234** (1984) 189;
 A. Manohar and G. Moore, *Nucl. Phys.* **B 243** (1984) 55;
 D. Espriu, E. de Rafael and J. Taron, *Nucl. Phys.* **B 345** (1990) 22.
- [2] V. Antonelli, S. Bertolini, M. Fabbrichesi and E.I. Lashin, *Nucl. Phys.* **B 469** (1996) 181.
- [3] S. Bertolini, J.O. Eeg and M. Fabbrichesi, *Nucl. Phys.* **B 476** (1996) 225.
- [4] T. Inami and C.S. Lim, *Prog. Theor. Phys.* **65** (1981) 297.
- [5] A.J. Buras, M. Jamin and P. H. Weisz, *Nucl. Phys.* **B 347** (1990) 491.
- [6] S. Herrlich and U. Nierste, *Nucl. Phys.* **B 419** (1994) 292.
- [7] S. Herrlich and U. Nierste, hep-ph/9604330, to appear in *Nucl. Phys.* **B** (1996).
- [8] L3 Coll., *Phys. Lett.* **B 248** (1990) 464, *Phys. Lett.* **B 257** (1991) 469;
 ALEPH Coll., *Phys. Lett.* **B 255** (1991) 623, *Phys. Lett.* **B 257** (1991) 479;
 DELPHI Coll., *Z. Physik* **C 54** (1992) 55;
 OPAL Coll., *Z. Physik* **C 55** (1992) 1;
 Mark-II Coll., *Phys. Rev. Lett.* **64** (1990) 987;
 SLD Coll., *Phys. Rev. Lett.* **71** (1993) 2528.
- [9] M.K. Gaillard and B.W. Lee, *Phys. Rev.* **D 10** (1974) 897.
- [10] A. Pich and J. Prades, *Phys. Lett.* **B 346** (1995) 342.
- [11] B. D. Gaiser, T. Tsao and M. B. Wise, *Ann. Phys. (NY)* **132** (1981) 66;
 A. J. Buras and J. -M. Gérard, *Nucl. Phys.* **B 264** (1986) 371.
- [12] J. F. Donoghue, E. Golowich and B. R. Holstein, *Phys. Lett.* **B 119** (1982) 412.
- [13] W. A. Bardeen, A. J. Buras and J. -M. Gérard, *Phys. Lett.* **B 211** (1988) 343.
- [14] A. Pich and E. de Rafael, *Nucl. Phys.* **B 358** (1991) 311.
- [15] C. Bruno, *Phys. Lett.* **B 320** (1994) 135.
- [16] A. Pich and E. de Rafael, *Phys. Lett.* **B 158** (1985) 477.

- [17] J. Prades, C. A. Domínguez, J. A. Peñarrocha, A. Pich and E. de Rafael, *Z. Physik C* **51** (1991) 287.
- [18] N. Bilić, C. A. Domínguez and B. Guberina, *Z. Physik C* **39** (1988) 351.
- [19] S. R. Sharpe, *Nucl. Phys. B* **34** (Proc. Suppl.) (1994) 403.
- [20] V. Antonelli, S. Bertolini, J.O. Eeg, M. Fabbrichesi and E.I. Lashin, *Nucl. Phys. B* **469** (1996) 143.
- [21] M. Ciuchini, E. Franco, G. Martinelli and L. Reina, *Nucl. Phys. B* **415** (1994) 403; *Phys. Lett. B* **301** (1993) 263.
- [22] A.J. Buras, M. Jamin, M.E. Lautenbacher and P.H. Weisz, *Nucl. Phys. B* **370** (1992) 69, (Addendum) *ibid.* **375** (1992) 501;
 A.J. Buras, M. Jamin, M.E. Lautenbacher and P.H. Weisz, *Nucl. Phys. B* **400** (1993) 37;
 A.J. Buras, M. Jamin and M.E. Lautenbacher, *Nucl. Phys. B* **400** (1993) 75;
 A.J. Buras, M. Jamin and M.E. Lautenbacher, *Nucl. Phys. B* **408** (1993) 209.
- [23] Particle Data group, *Phys. Rev. D* **50** (1994) 1173.
- [24] M.A. Shifman, A.I. Vainshtain and V.I. Zakharov, *Nucl. Phys. B* **120** (1977) 316;
 F.J. Gilman and M.B. Wise, *Phys. Rev. D* **20** (1979) 2392;
 J. Bijnens and M.B. Wise, *Phys. Lett. B* **137** (1984) 245;
 M. Lusignoli, *Nucl. Phys. B* **325** (1989) 33.
- [25] J. Gasser and H. Leutwyler, *Ann. Phys. (NY)* **158** (1984) 142, *Nucl. Phys. B* **250** (1985) 465,517,539;
 see also : A.Pich, *Introduction to Chiral Perturbation Theory*, Lectures at V Mexican School of Particles and Fields 1992, hep-ph 9308351.
- [26] J. F. Donoghue, E. Golowich and B. R. Holstein, *Phys. Lett. B* **135** (1984) 481.
- [27] I. I. Bigi and A. I. Sanda, *Phys. Lett. B* **148** (1984) 205.
- [28] P. Cea and G. Nardulli, *Phys. Lett. B* **152** (1985) 25.
- [29] M. R. Pennington, *Phys. Lett. B* **153** (1985) 439.
- [30] A. J. Buras and J. -M. Gérard, *Nucl. Phys. B* **264** (1986) 371.
- [31] K. Terasaki and S. Oneda, Preprint. RRK, 89-21 (1989).
- [32] T. Kurimoto, *Prog. Theor. Phys.* **84** (1990) 658.
- [33] J. Bijnens, J. -M. Gérard and G. Klein *Phys. Lett. B* **257** (1991) 191.

- [34] M. Fabbrichesi and E.I. Lashin, hep-ph/9606279, to appear in *Phys. Lett. B* (1996).
- [35] L. Wolfenstein, *Nucl. Phys. B* **160** (1979) 501.
- [36] V. Antonelli, *Aspects of Kaon Physics in Chiral Perturbation Theory and Chiral Quark Model*, Ph.D. Thesis (SISSA, Trieste, October 1996);
E.I. Lashin, *Chiral Quark Model for Kaons*, Ph.D. Thesis (SISSA, Trieste, October 1996), unpublished.